

# THE JOURNAL OF PHYSICAL CHEMISTRY C

Subscriber access provided by UNIV OF DURHAM

C: Surfaces, Interfaces, Porous Materials, and Catalysis

## Bromide Adsorption on Pt(111) Over a Wide Range of pH: Cyclic Voltammetry and CO Displacement Experiments

Gisele Afonso Bento Mello, Valentin Briega-Martos, Victor Climent, and Juan M. Feliu

*J. Phys. Chem. C*, **Just Accepted Manuscript** • DOI: 10.1021/acs.jpcc.8b05685 • Publication Date (Web): 23 Jul 2018Downloaded from <http://pubs.acs.org> on July 23, 2018

### Just Accepted

“Just Accepted” manuscripts have been peer-reviewed and accepted for publication. They are posted online prior to technical editing, formatting for publication and author proofing. The American Chemical Society provides “Just Accepted” as a service to the research community to expedite the dissemination of scientific material as soon as possible after acceptance. “Just Accepted” manuscripts appear in full in PDF format accompanied by an HTML abstract. “Just Accepted” manuscripts have been fully peer reviewed, but should not be considered the official version of record. They are citable by the Digital Object Identifier (DOI®). “Just Accepted” is an optional service offered to authors. Therefore, the “Just Accepted” Web site may not include all articles that will be published in the journal. After a manuscript is technically edited and formatted, it will be removed from the “Just Accepted” Web site and published as an ASAP article. Note that technical editing may introduce minor changes to the manuscript text and/or graphics which could affect content, and all legal disclaimers and ethical guidelines that apply to the journal pertain. ACS cannot be held responsible for errors or consequences arising from the use of information contained in these “Just Accepted” manuscripts.



ACS Publications

is published by the American Chemical Society, 1155 Sixteenth Street N.W.,  
Washington, DC 20036Published by American Chemical Society. Copyright © American Chemical Society.  
However, no copyright claim is made to original U.S. Government works, or works  
produced by employees of any Commonwealth realm Crown government in the course  
of their duties.

# Bromide Adsorption on Pt(111) over a Wide Range of pH: Cyclic Voltammetry and CO Displacement Experiments

*Gisele A. B. Mello<sup>1,2</sup>, Valentín Briega-Martos<sup>1</sup>, Víctor Climent<sup>1\*</sup>, Juan M. Feliu<sup>1\*</sup>*

<sup>1</sup>Instituto de Electroquímica, Universidad de Alicante, Apdo. 99, E-03080 Alicante, Spain.

<sup>2</sup> Curso de Licenciatura em Química, Instituto de Ciências da Educação, Universidade Federal do Oeste do Pará, Avenida Marechal Rondon, s/n, CEP 68040-070, Santarém, PA, Brazil.

\*Corresponding authors: [victor.climent@ua.es](mailto:victor.climent@ua.es), [juan.feliu@ua.es](mailto:juan.feliu@ua.es)

## ABSTRACT

Bromide adsorption on Pt(111) is investigated by means of cyclic voltammetry and CO displacement experiments at different pH values. In acidic pH bromide adsorption is strongly overlapped with hydrogen desorption process. However, as the pH increases, hydrogen adsorption process displaces towards negative potentials while bromide adsorption remains nearly in the same potential region. In consequence, both processes decouple at higher pH values. The structural transition from Pt(111)-(1×1) to Pt(111)(3×3)-4Br is pH independent, in the SHE scale, and not observed for pH > 9.1. Values of  $p_{ztc}$  are extracted from the combination of voltammetric and CO displaced charges. An alternative approach to obtain charge curves is based on the coincidence of the curves the structural transition characteristic of the bromide adlayer completion.  $P_{ztc}$  values obtained from different approaches with and without bromide are compared and their dependence on pH discussed. A thermodynamic analysis is carried out to obtain hydrogen Gibbs excess and charge number from the Esin Markov analysis.

## 1. INTRODUCTION

The knowledge of the properties of the metal-electrolyte interface has fundamental importance in electrochemistry. It is well established that the rate determining step of all electrocatalytic reactions necessarily involves adsorbed species or at least a specific interaction between reactants or intermediates and the electrocatalytic surface. Such interactions are expected to be extremely sensitive to the interfacial charge and/or the existence of co-adsorption phenomena. For that reason, quantifying the amount of charge separation at the electrochemical double layer is extremely important to rationalize the electrocatalytic phenomena. For this, the fundamental property that should be investigated to relate the electrode potential, which is the directly measurable quantity, with the interfacial charge, is the potential zero charge (pzc).<sup>1-5</sup> Two different types of pzc can be defined at platinum electrodes, the potential of zero free charge (pzfc) and the potential of zero total charge (pztc). While the free charge considers the true electronic excess charge on the metal, compensated by the ionic charge on the electrolyte, the only accessible quantity is the total charge which includes both capacitive and pseudo-capacitive (faradaic) contributions. The pztc can be measured with the CO displacement experiments,<sup>1,2,4-9</sup> while the pzfc can only be calculated in some particular cases from the pztc by using some additional assumptions<sup>10</sup>. Besides, the location of the pzfc can be inferred from some indirect measurements like the reorientation of interfacial water molecules monitored by laser-induced temperature jump experiments.<sup>11-13</sup>

When anion specific adsorption takes place on the electrode surface it is extremely important to determine the charge transfer characteristics involved in this process, since it implies changes in the pztc and it also promotes electrode surface modifications.<sup>3,14</sup> The structural adlayer of the adsorbed anion can be “incommensurate”

1  
2  
3 or “commensurate” depending on what type of interaction is stronger, as pointed out by  
4  
5 Lucas *et al.*<sup>15</sup> On the one hand, if the interaction between nearby adatoms is stronger,  
6  
7 the structural adlayer will be “incommensurate”. On the other hand, if the adatom-  
8  
9 substrate interaction is stronger, then structural adlayer will be “commensurate”.

10  
11 Bromide adsorption on Pt(111) was subject of investigation by Hubbard’s group<sup>16-</sup>  
12  
13 <sup>18</sup> providing precious information about the characterization of the formed adlayers.  
14  
15 UHV measurements by LEED and Auger spectroscopy were employed to characterize  
16  
17 the adlayer, and these works opened the way for further similar investigations.<sup>3,19-22</sup> The  
18  
19 Pt(111)-Br<sub>ads</sub> adlayer was also characterized by STM<sup>3,23</sup> and surface X-ray scattering.<sup>19</sup>  
20  
21 The bromide adlayers can be formed either from bromide solutions or bromide vapors.<sup>3</sup>  
22  
23 A structural transition at 0.25 V vs. RHE in 0.1 M HClO<sub>4</sub> was observed.<sup>3,18,23</sup> It was  
24  
25 first proposed that this feature corresponds to the change from a Pt(111)-(3×3)-4Br  
26  
27 adlattice at high potentials to a Pt(111)-(4×4)-7Br adlattice at low potentials,<sup>18</sup> but Itaya  
28  
29 *et al.* observed an incommensurate Pt(111)-(1×1) structure instead of Pt(111)-(4×4)-  
30  
31 7Br.<sup>23</sup> Independently of the technique used for the characterization of the Pt(111)-Br<sub>ads</sub>  
32  
33 adlayer, it was shown that the Pt(111)-(3×3)-4Br structure is dense and the bromine  
34  
35 adatoms are arranged in a closed-packed hexagonal layer, where the Br-Br distance is  
36  
37 close to van der Waals diameter of bromine. They pointed out also that these adlayers  
38  
39 are ordered preferentially along the directions of the substrate densest rows.<sup>3,16-18,24</sup>  
40  
41 Lucas *et al.*<sup>19</sup> proposed similar observations, although in these studies they observed  
42  
43 that the (3×3) adlayer structure was incommensurate, whereas Orts *et al.*<sup>3</sup> proposed it as  
44  
45 commensurate.  
46  
47  
48  
49

50  
51 In the present work, the knowledge about bromide adsorption on Pt(111) is  
52  
53 extended by performing cyclic voltammetry and CO displacement experiments in  
54  
55 solutions with a wide range of pH values.  
56  
57  
58  
59  
60

## 2. EXPERIMENTAL SECTION

Experiments were performed in a glass electrochemical cell with three electrodes following the general procedure described in Korzeniewski *et al.*<sup>25</sup> Pt(111) working electrode was prepared from a small Pt bead ca. 2 mm in diameter according to the procedure described by Clavilier *et al.*<sup>26</sup> The reference electrode was a reversible hydrogen electrode (RHE) in all cases, although some results are presented vs the SHE in some figures. The counter electrode was a platinum coiled wire cleaned by flame annealing and quenched with ultrapure water.

Working solutions with pH values lower than 3 were prepared by using HClO<sub>4</sub> (Merck, for analysis) and KClO<sub>4</sub> (EMSURE ACS for analysis 99.5%-100.5%, Merck). For pH values ranging from 3 to 9, phosphate buffer solutions were employed (Na<sub>2</sub>HPO<sub>4</sub> and NaH<sub>2</sub>PO<sub>4</sub>, traceSELECT<sup>®</sup>, Fluka Analytical). Alkaline solutions were prepared with NaOH (99.99%, trace metals, Sigma-Aldrich) and KClO<sub>4</sub>. Bromide adsorption was investigated by using KBr (Merck, Suprapur, 99.99%). Ultrapure water (Elga PureLab Ultra, 18.2 MΩ cm) was employed for glassware cleaning and preparation of all the working solutions. Ar, H<sub>2</sub> and CO (N50, Air Liquide) were also employed. CO displacement experiments were performed as described elsewhere.<sup>4,7-9</sup>

The electrode potentials were controlled using a waveform generator (PARC 175, EG&G) together with a potentiostat (eDAQ 401) and a digital recorder (eDAQ ED401). All the experiments were carried out at room temperature.

## 3. RESULTS AND DISCUSSION

### *Bromide adsorption on Pt(111)*

Cyclic voltammetric profiles for Pt(111) in the absence of bromide and in the presence of 10<sup>-2</sup> M Br<sup>-</sup> at pH values from 1.2 to 11.5 are shown in Fig. 1. In the case of

1  
2  
3 the blank voltammeteries without bromide, the hydrogen adsorption/desorption region  
4 appears between 0.06 V and 0.4 V (vs RHE) for all the experiments in the complete pH  
5 range investigated.<sup>27-29</sup> However, the voltammetric peaks associated with the (100) and  
6 (110) defects shift with pH with a non-Nernstian behavior.<sup>28,29</sup> Such shift has been  
7 recently attributed to the presence of cations in the buffer solution.<sup>30</sup> When no anion  
8 specific adsorption is present, the adsorption/desorption feature of hydroxyl anions is  
9 observed at high potentials, while in the presence of phosphate anions this region is  
10 displaced to more negative potentials and different irreversible sharp peaks appear due  
11 to the adsorption of phosphate species.<sup>28</sup> It is important to take into account that the  $pK_a$   
12 for the phosphate species at the metal|solution interface are much lower than their  
13 values for the same species in the bulk solution.<sup>31</sup> Therefore, phosphate species that  
14 would not be found in the bulk solution at a certain pH could be present at the interface.

15  
16  
17  
18  
19  
20  
21  
22  
23  
24  
25  
26  
27  
28  
29 In the presence of  $10^{-2}$  M KBr the voltammetric profiles are significantly different  
30 because of the specific adsorption of bromide anions.<sup>3,7,9</sup> Symmetrical curves are  
31 obtained in both positive and negative-going sweeps for all the pH values. In the case of  
32 0.1 M HClO<sub>4</sub> (pH = 1.2) most of the voltammetric charge appears at potentials lower  
33 than 0.4 V vs. RHE and two main peaks can be observed at 0.18 V and 0.23 V vs.  
34 RHE.<sup>3</sup> The measured charges at low potentials arise from both hydrogen  
35 adsorption/desorption and bromide desorption/adsorption on the platinum surface.<sup>15,20,22</sup>  
36  
37  
38  
39  
40  
41  
42  
43  
44  
45  
46  
47  
48  
49  
50  
51  
52  
53  
54  
55  
56  
57  
58  
59  
60  
In acid solutions, these processes overlap significantly,<sup>3</sup> but, as the pH increases, the  
bromide adsorption moves to more positive potential values (in the RHE scale),  
separating from the hydrogen adsorption/desorption region. Bromide adsorption can  
also be inferred by the suppression of the OH<sup>-</sup> desorption/adsorption region, as observed  
for other specifically adsorbed anions.<sup>5,32</sup> This feature is completely suppressed at acidic  
pH values, but, as the solution pH is increased, the adsorption strength of bromide

anions decreases, and, for pH = 11.5, the hydroxyl anions desorption/adsorption region remains practically unchanged.<sup>18,22</sup> In addition, the first peak associated with bromide adsorption becomes broader and diminishes drastically its intensity as the pH of the solution is increased, which indicates that the adsorption strength of Br<sup>-</sup> is decreasing.

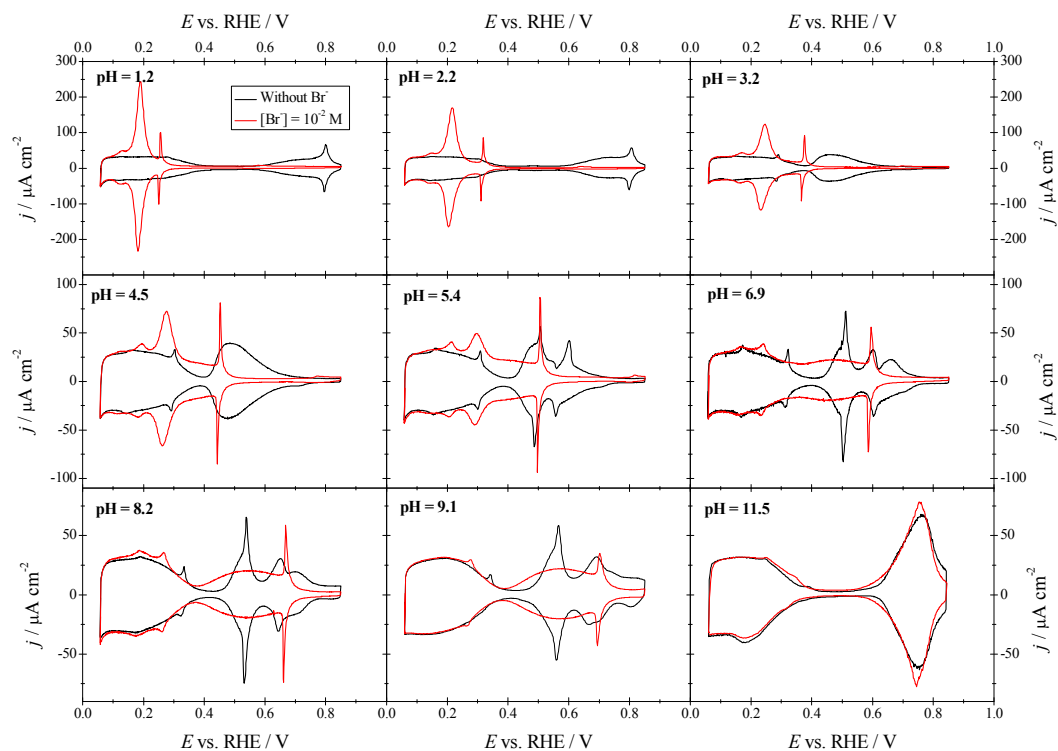


Figure 1: Voltammetric profiles for Pt(111) in different solutions with pH values ranging from 1.2 to 11.5 in the absence of KBr (black line) and in presence of  $10^{-2}$  KBr (red line). Scan rate:  $50 \text{ mV s}^{-1}$ .

The sharp peak at 0.18 V vs. RHE at pH = 1.2 is associated to the structural transition from Pt(111)-(1×1) (or Pt(111)(4×4)-7Br) to Pt(111)(3×3)-4Br (in the positive-going scan), which involves the oxidative adsorption of Br<sup>-</sup> and the reconstruction of the bromide adlattice.<sup>3,16-18,23,24</sup> It is important to remark that the peak potential of this spike

is pH independent in the SHE scale (as can be seen in Figure 2), suggesting that this structural transition does not involve the displacement of hydrogen.<sup>18,22</sup> This reconstruction peak becomes markedly broader and lower at pH = 9.1, while at pH = 11.5 completely vanishes. This reinforces the idea that bromide adsorption is strongly inhibited by the competitive adsorption of OH<sub>ads</sub>. In this sense, pH = 9.1 would be the pH limit in which bromide anions could adsorb promoting the structural transition (Figure 2). The pH-independent behavior of the structural transition spike for bromide differs from H<sub>2</sub>SO<sub>4</sub> solutions because in the latter case the adsorption of sulfate also implies the transfer of protons.<sup>33</sup>

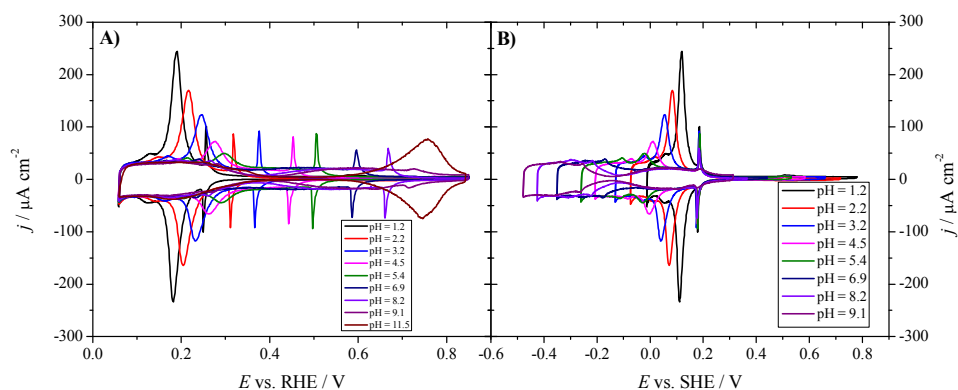


Figure 2: Voltammetric profiles for Pt(111) in different solutions with pH values ranging from 1.2 to 11.5 in presence of 10<sup>-2</sup> M KBr in the RHE scale (A) and in the SHE scale (B). Scan rate: 50 mV s<sup>-1</sup>.

The curves plotting total charge as a function of potential for some of the studied pH values are shown in Figure 3A. These curves were obtained from the integration of the cyclic voltammogram in the presence of bromide using the total charge obtained from CO displacement experiments performed at 0.1 V vs. RHE as the integration constant.<sup>1,5,34</sup> Displaced charges with CO were corrected to consider the remaining charge on the interface after CO adsorption.<sup>35</sup> From these plots the potential of zero total charge (pztc) can be estimated as the point where the curve crosses the potential



1  
2  
3 axis, i.e. the potential value at  $y=0$ .<sup>2,34,36,37</sup> As usual, there is an increase in the charge  
4  
5 densities with potential (Figure 3A). The negative charge at lower potentials is mainly  
6  
7 due to the reductive hydrogen adsorption. The inflection points mark the potential range  
8  
9 where bromide adsorption takes place. The first inflection at lower potentials  
10  
11 (overlapped with the hydrogen adsorption process) marks the onset of bromide  
12  
13 adsorption while the one at higher potentials similar in shape to sulfate adsorption,  
14  
15 marks the completion of the adlayer, which finishes in the sharp spike, except for pH  
16  
17 9.1 in which the sharp spike is nearly absent. The positive charges above 0.12 V in the  
18  
19 most acidic solution are associated to the dominance of the oxidative adsorption of  
20  
21 bromide species. At increasing pH, the slope of the charge/potential profiles decreases,  
22  
23 demonstrating the separation of bromide adsorption process as a function of pH: in  
24  
25 more acid solutions the bromide adsorption occurs in a competitive process with  
26  
27 hydrogen desorption and increasing the pH the bromide adsorption occurs at higher  
28  
29 relative potentials, on a surface almost free of adsorbed hydrogen, where mainly water  
30  
31 is in contact with the metal. Figure 3B shows a comparison between the pztc values for  
32  
33 phosphate buffer solutions in presence and in absence of bromide. Note that increasing  
34  
35 the pH, the pztc values are shifted towards less positive values when  $10^{-2}$  M  $\text{Br}^-$  is  
36  
37 present, which indicates that in acid medium bromide adsorption is stronger than in  
38  
39 alkaline medium. The bromide structural transition takes place at higher potentials than  
40  
41 the pztc for all cases. It is noteworthy that the ptzc for pH 6.9 and 9.1 are very close,  
42  
43 although the bromide adsorption in pH 9.1 is strongly inhibited in comparison to pH  
44  
45 6.9. This indicates that pH 9.1 seems to be the pH limit in which the competition with  
46  
47 the adsorption of oxygenated species prevents these surface phenomena promoted by  
48  
49 bromide. In the absence of bromide anions a monotonic trend is observed since different  
50  
51 phosphate species are participating depending on the pH. However, it can be seen that  
52  
53  
54  
55  
56  
57  
58  
59  
60

1  
2  
3 the pztc always tends to approach the value corresponding to the absence of specific  
4  
5 anion adsorption at very high pH (Figure 3B).  
6  
7

8  
9 It is important to highlight that in presence of strongly adsorbed anions, the  
10  
11 interfacial properties at the highest potential range should be pH independent, since the  
12  
13 adsorption of oxygenated species is suppressed by anion adsorption (Figure 1). Hence,  
14  
15 in the particular region where the Br<sup>-</sup> adlayer is completed, no other contributions are  
16  
17 involved and the charge at the interface should be pH independent.<sup>32</sup> The coincidence of  
18  
19 the voltammetric curves between 0.12 V – 0.17 V (vs. SHE) in the pH range between  
20  
21 3.4 and 9.1 (Figure 2) illustrates this idea. Also, the charge curves in figure 3A  
22  
23 demonstrate the independence of the interfacial properties on pH in the highest potential  
24  
25 range. It must be remarked that this is obtained as an experimental result from the  
26  
27 combination of current integration and displaced charges. An alternative approach  
28  
29 would be to impose the coincidence of the curves at a potential higher than the spike at  
30  
31 0.15 V. In this way, the relative position of the charge curves could be elucidated  
32  
33 without the use of CO displaced charges as integration constant. We would only need  
34  
35 one integration constant for one of the curves to obtain the absolute position of all the  
36  
37 curves at the different pHs. On the other hand, charge curves with and without bromide  
38  
39 should coincide in the lowest potential range where bromide is completely desorbed and  
40  
41 the properties of the interphase are dominated by hydrogen adsorption. This is  
42  
43 illustrated in figure 4. In this figure all the curves integrated from the voltammograms  
44  
45 with bromide in different pH solutions are adjusted to coincide at 0.3 V SHE. Then,  
46  
47 every curve recorded in the absence of bromide is made to coincide with the  
48  
49 corresponding curve recorded at the same pH but with bromide at 0.1 V RHE (this  
50  
51 potential shifts in the SHE scale). In this way, the relative position of all the curves is  
52  
53  
54  
55  
56  
57  
58  
59  
60

adjusted. Finally, one single integration constant would only be needed to adjust the absolute position of all the curves with and without bromide and for every pH. This integration constant has been taken as  $-154 \mu\text{Ccm}^{-2}$  at 0.1 V RHE for  $\text{pH}=1.2$ . This number corresponds to a displaced charge of  $-141 \mu\text{Ccm}^{-2}$  plus a correction due to the remaining charge on the CO covered surface after the displacement experiment of  $-13 \mu\text{Ccm}^{-2}$ .

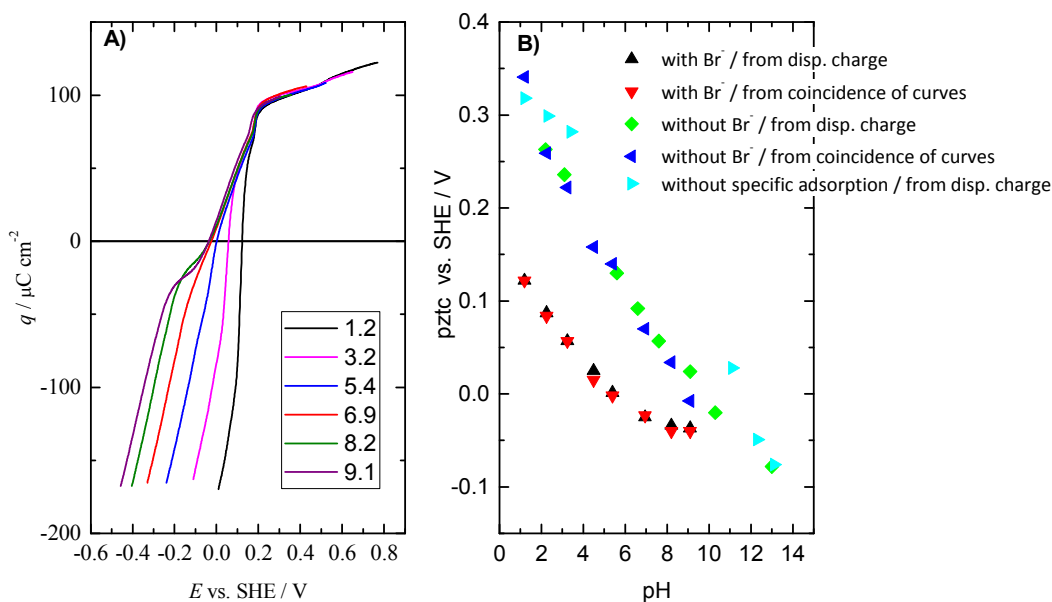


Figure 3: Charge curves obtained from the integration of the corresponding voltammograms with  $10^{-2}$  M KBr and using the charge obtained by CO displacement at 0.1 V as the integration constant (A) and comparison of the potential of zero charge at different pH values for different compositions (B).

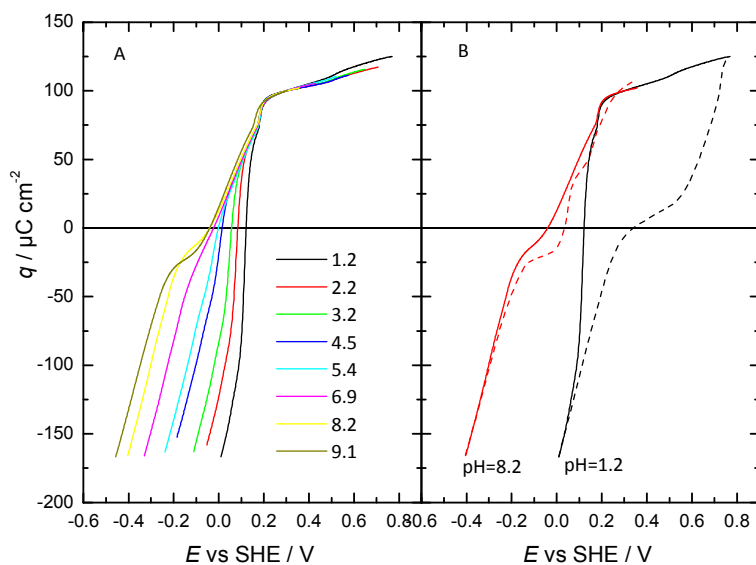


Figure 4: Charge curves obtained from the integration of the corresponding voltammograms with  $10^{-2}$  M KBr and from the coincidence of the curves (A). Exemplification of the method employed to establish the relative position of charge curves (i.e., integration constant) from the coincidence with (solid lines) and without (dashed lines) bromide in the low potential region (at 0.1 V vs. RHE) (B).

In this way, the dependence of pztc values with pH can be accurately obtained with less experimental uncertainty than the one associated with the CO displacement. It should be stressed that one of the uncertainties associated with the CO displacement, the dependence of the correction for the remaining charge on the CO covered surface with the pH, is avoided in this approach since only one integration constant is used at a single pH value. The same approach has been previously used to obtain information of the interfacial properties in a much narrow pH range.<sup>32,38</sup> From the result plotted in figure 4, the pztc values for solutions with and without bromide can be easily obtained from the intersection with the  $q=0$  axis. The results obtained with this approach are plotted in figure 3B, together with the values obtained with the charge displacement technique, demonstrating the good agreement between both approaches.

Because the accuracy in the determination of the relative position of the curves is better with this second approach, we adopt it for the analysis that follows.

The plot of pztc vs. pH is a particular case of an Esin Markov plot. In general, the Esin Markov coefficient is defined as the variation of the potential at constant charge as a function of the chemical potential of one species in solution. Under the light of the electrocapillary equation this can be related with the formal charge transfer number at constant charge:

$$d\xi = Edq - \Gamma d\mu_{H^+} \quad (1)$$

Where  $\xi$  is the Parsons function defined as  $\xi = \gamma + qE$ . According to this exact differential, based on the equality of cross partial derivatives, we obtain the desired relationship:

$$\left(\frac{\partial E}{\partial \mu_{H^+}}\right)_q = -\frac{1}{RT} \left(\frac{\partial E}{\partial pH}\right)_q = -\left(\frac{\partial \Gamma_{H^+}}{\partial q}\right)_\mu \quad (2)$$

Where

$$n' = -\frac{1}{F} \left(\frac{\partial q}{\partial \Gamma_{H^+}}\right)_\mu = -\frac{RT \ln 10}{F} \left(\frac{\partial E}{\partial pH}\right)_q^{-1} \quad (3)$$

is the formal partial charge number for  $H^+$  adsorption.

From the curves of figure 4A we can take horizontal cuts to obtain values of potential for different values of constant charge to plot them as a function of the pH. The result is shown for some selected charge value in figure 5A and B for solutions with and without bromide, respectively.

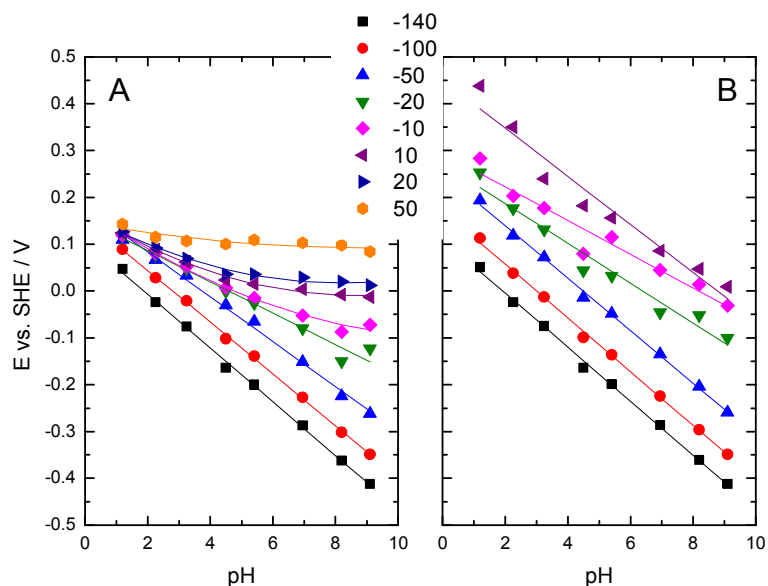


Figure 5: Plot of potential of constant charge as a function of pH for solutions with (A) and without (B) bromide. The lines represent the best fit to either a straight line or to a parabola (with bromide for  $q > -16 \mu\text{Ccm}^{-2}$ ).

From the slope of the plots, the charge numbers involved in the adsorption of hydrogen can be calculated. For the curves obtained in the presence of bromide, at charges higher than  $-16 \mu\text{Ccm}^{-2}$  the plots clearly deviates from straight lines and a parabolic fit was used to extract the slopes. Such deviation from linearity is a consequence of the coadsorption of bromide with hydrogen, since degree of the overlap of both processes changes with pH. In this way, for charges above  $-20 \mu\text{Ccm}^{-2}$ , while hydrogen adsorption process is already finished in the curves with highest pH, there is still a pH dependence for the curves with lowest pH. Regarding the plot in the absence of bromide the plot shows parallel straight lines, indicating that the charge numbers in this case are relatively insensitive to either pH or charge (potential).

The charge numbers calculated in this way are plotted as a function of the charge in figure 6:

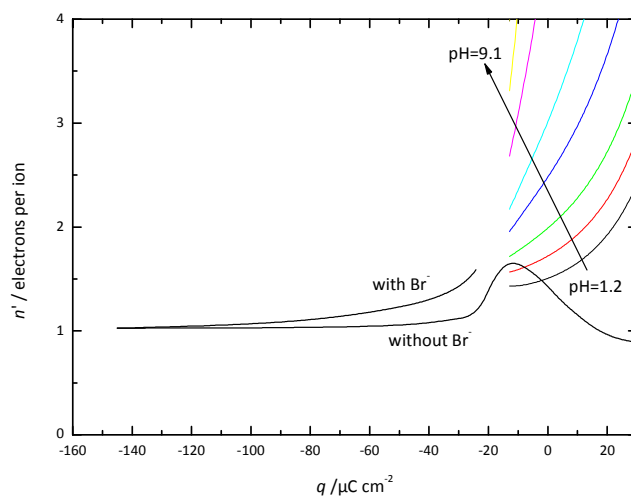


Figure 6: Charge numbers at constant chemical potential obtained from the inverse of Esin Markov coefficient plotted as a function of the charge. To obtain the slopes from the curves with bromide, linear fits are used for  $q < -20 \mu\text{Ccm}^{-2}$  and quadratic fit for  $q > -20 \mu\text{Ccm}^{-2}$ .

Charge numbers involved in hydrogen adsorption in the absence of bromide are very close to one in accordance with previous calculations.<sup>39</sup> This suggest that  $\text{H}^+$  are totally discharged upon adsorption. In the case of solutions that contain bromide, charge number tend to one at the lowest charge (potential) values but small deviations from unity take place. This reflects the coadsorption effect of bromide as has been demonstrated before for other anions. In the presence of coadsorption:

$$n' = -\frac{1}{F} \left( \frac{\partial q}{\partial \Gamma_{\text{H}}} \right)_{\mu_{\text{H}^+}} = -\frac{1}{F} \left( \frac{\partial q}{\partial \Gamma_{\text{H}}} \right)_{\mu_{\text{H}^+}, \Gamma_{\text{Br}}} - \frac{1}{F} \left( \frac{\partial q}{\partial \Gamma_{\text{Br}}} \right)_{\mu_{\text{H}^+}, \Gamma_{\text{H}}} \left( \frac{\partial \Gamma_{\text{Br}}}{\partial \Gamma_{\text{H}}} \right)_{\mu_{\text{H}^+}} \quad (4)$$

Since  $\left( \frac{\partial q}{\partial \Gamma_{\text{Br}}} \right)_{\mu_{\text{H}^+}, \Gamma_{\text{H}}}$  is always positive, for the adsorption of an anion,  $\left( \frac{\partial \Gamma_{\text{Br}}}{\partial \Gamma_{\text{H}}} \right)_{\mu_{\text{H}^+}}$  must be negative, as corresponds to a competitive adsorption phenomena.

Additional information can be obtained from equation (1). According to this equation, hydrogen coverage,  $\Gamma_{H^+}$  can be obtained by differentiating  $\xi$ :

$$\Gamma_H = - \left( \frac{\partial \xi}{\partial \mu_{H^+}} \right)_q = \frac{1}{RT \ln 10} \left( \frac{\partial \xi}{\partial pH} \right)_q \quad (5)$$

Values of  $\xi$  can be obtained from integration of the potential as a function of charge, except for an integration constant. Although this integration constant is unknown, it can be assumed independent of the pH at sufficiently high potential (charge) values. Following this approach, the potential was integrated as a function of charge and all the resulting curves were shifted to make them coincide at  $q=100 \mu\text{Ccm}^{-2}$ . The result is shown in figure 7:

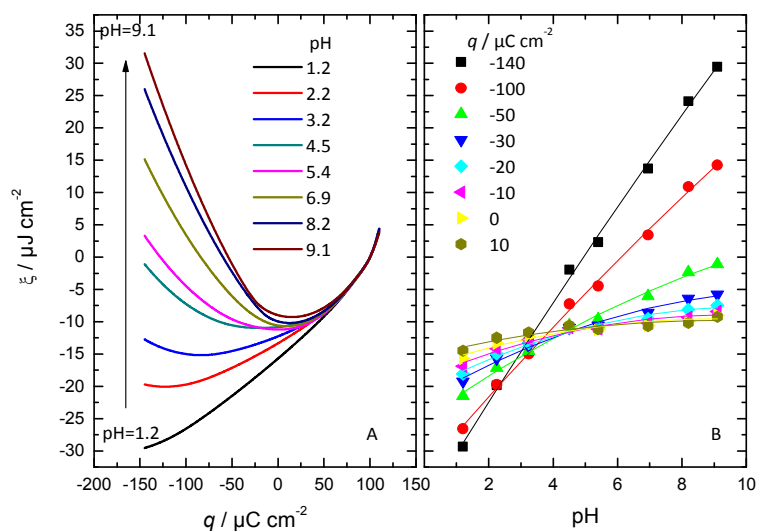


Figure 7: plot of Parsons function,  $\xi$ , A) as a function of charge for different pH or B) as a function of pH for different values of charge, as integrated for the solutions containing bromide.

According to equation (5) hydrogen coverage can be obtained from the slopes of plots in figure 7B. Although these plots are nearly linear they exhibit some curvature,



especially those at higher charge, indicating that the low coverages of hydrogen depend slightly on pH. For this reason, both quadratic and linear fits were used to extract the slopes and the results are compared in figure 8.

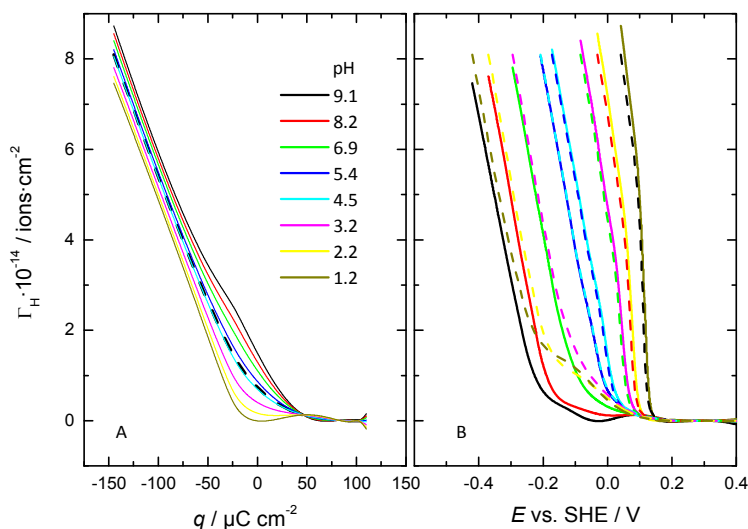


Figure 8: Plot of the surface excess as a function of A) charge and B) potential. Dashed lines correspond to the result obtained with a linear fit, while solid lines are results obtained with quadratic fit.

The maximum hydrogen coverage obtained is around  $8.5 \cdot 10^{14} \text{ cm}^{-2}$  what is equivalent to  $136 \text{ } \mu\text{Ccm}^{-2}$  in reasonable agreement with the value obtained with voltammetry. While there is little difference between the quadratic and linear fit for high coverage values, at low coverages, the results from the quadratic fit seem to produce better results. It is also noteworthy the change of slope in the curves for the lower pH in figure 8B, which signals the potential where bromide adsorption forces the displacement of the remaining adsorbed hydrogen.

#### 4. CONCLUSIONS

In this work the adsorption of bromide adlayers on Pt(111) at different pH values is studied. Results show that when bromide anions are present the same results are obtained independently of the presence of other possible species that could adsorb specifically such as phosphate or sulphate anions. It is observed that the sharp peak from the structural transition from Pt(111)-(1×1) to Pt(111)-(3×3)-4Br is pH independent and pH = 9.1 seems to be the limit in which the adsorption of oxygenated species does not prevent this surface reconstruction. CO displacement experiments point out that the pztc is displaced to more negative values as the pH is increased, indicating that bromide adsorption is stronger in acid than in alkaline media.

Charge curves have been obtained from an alternative method based on the coincidence of charge for all pH solutions at the potential where the bromide adlayer is complete (at 0.3 V vs. SHE). In this way, the curves with and without bromide for different pH solutions can be compared. The result is in excellent agreement with that obtained from CO displacement and overcomes the uncertainty inherent to the latter technique regarding the remaining charge on the CO covered surface. The thermodynamic analysis allowed calculation of hydrogen coverage and charge number under different pH conditions. The Esin Markov analysis signals the coadsorption of bromide and hydrogen and that the degree of overlap of both processes changes with pH.

#### ACKNOWLEDGEMENTS

This work has been financially supported by the MCINN-FEDER (Spain) through project CTQ2016-76221-P. VBM thankfully acknowledges to MINECO the award of a predoctoral grant (BES-2014-068176, project CTQ2013-44803-P). GABM thanks the post-doctorate fellowship from CNPq (grant no. PDE 233268/2014-6).

## REFERENCES

- (1) Cuesta, A. Measurement of the surface charge density of CO-saturated Pt(111) electrodes as a function of potential: The potential of zero charge of Pt(111). *Surf. Sci.* **2004**, *572*, 11-22.
- (2) Climent, V.; Gómez, R.; Feliu, J. M. Effect of increasing amount of steps on the potential of zero total charge of Pt(111) electrodes. *Electrochim. Acta* **1999**, *45*, 629-637.
- (3) Orts, J. M.; Gómez, R.; Feliu, J. M.; Aldaz, A.; Clavilier, J. Nature of Br adlayers on Pt(111) single-crystal surfaces. Voltammetric, charge displacement, and ex situ STM experiments. *J. Phys. Chem.* **1996**, *100*, 2334-2344.
- (4) Rizo, R.; Sitta, E.; Herrero, E.; Climent, V.; Feliu, J. M. Towards the understanding of the interfacial pH scale at Pt(111) electrodes. *Electrochim. Acta* **2015**, *162*, 138-145.
- (5) Martínez-Hincapié, R.; Sebastián-Pascual, P.; Climent, V.; Feliu, J. M. Exploring the interfacial neutral pH region of Pt(111) electrodes. *Electrochem. Commun.* **2015**, *58*, 62-64.
- (6) Clavilier, J.; Orts, J. M.; Gómez, R.; Feliu, J. M.; Aldaz, A. On the Nature of the Charged Species Displaced by CO Adsorption from Platinum Oriented Electrodes in Sulphuric Acid Solution; Conway, B. E., Jerkiewicz, G., Eds.; The Electrochemical Society, INC.: Pennington, NJ, 1994; Vol. 94-21; pp 167-183.
- (7) Orts, J. M.; Gómez, R.; Feliu, J. M.; Aldaz, A.; Clavilier, J. Potentiostatic charge displacement by exchanging adsorbed species on Pt(111) electrodes—acidic electrolytes with specific anion adsorption *Electrochim. Acta* **1994**, *39*, 1519-1524.
- (8) Clavilier, J.; Albalat, R.; Gómez, R.; Orts, J. M.; Feliu, J. M.; Aldaz, A. Study of the charge displacement at constant potential during CO adsorption on Pt(110) and Pt(111) electrodes in contact with a perchloric acid solution. *J. Electroanal. Chem.* **1992**, *330*, 489-497.
- (9) Clavilier, J.; Albalat, R.; Gómez, R.; Orts, J. M.; Feliu, J. M. Displacement of adsorbed iodine on platinum single-crystal electrodes by irreversible adsorption of CO at controlled potential. *J. Electroanal. Chem.* **1993**, *360*, 325-335.
- (10) Climent, V.; Gómez, R.; Orts, J. M.; Aldaz, A.; Feliu, J. M. *The potential of zero total charge of single-crystal electrodes of platinum group metals*; The Electrochemical Society, Inc.: Pennington, NJ, 1997; Vol. 97-17; pp 222-237.
- (11) Garcia-Araez, N.; Climent, V.; Feliu, J. Potential-dependent water orientation on Pt(111), Pt(100), and Pt(110), as inferred from laser-pulsed Experiments. Electrostatic and chemical effects. *J. Phys. Chem. C* **2009**, *113*, 9290-9304.
- (12) Garcia-Araez, N.; Climent, V.; Feliu, J. M. Potential-dependent water orientation on Pt(111) stepped surfaces from laser-pulsed experiments. *Electrochim. Acta* **2009**, *54*, 966-977.
- (13) Sebastián, P.; Martínez-Hincapié, R.; Climent, V.; Feliu, J. M. Study of the Pt(111) | electrolyte interface in the region close to neutral pH solutions by the laser induced temperature jump technique. *Electrochim. Acta* **2017**, *228*, 667-676.
- (14) Gómez, C. R.; Orts, J. M.; Aldaz, A.; Feliu, J. M. *The potential of zero total charge of single crystal electrodes of platinum group metals*. In *Elec Soc S*; Korzeniewski, C., Conway, B. E., Eds., 1997; Vol. 97; pp 222-237.
- (15) Lucas, C. A.; Markovic, N. M.; Ross, P. N. Adsorption of halide anions at the Pt(111)-solution interface studied by in situ surface x-ray scattering. *Phys. Rev. B* **1997**, *55*, 7964-7971.
- (16) Garwood Jr., G. A.; Hubbard, A. T. Superlattices formed by interaction of hydrogen bromide and hydrogen chloride with Pt(111) and Pt(100) studied by LEED, Auger and thermal desorption mass spectroscopy. *Surf. Sci.* **1981**, *112*, 281-305.
- (17) Stickney, J. L.; Rosasco, S. D.; Salaita, G. N.; Hubbard, A. T. Ordered ionic layers formed on platinum(111) from aqueous solutions. *Langmuir* **1985**, *1*, 66-71.

- 1  
2  
3 (18) Salaita, G. N.; Stern, D. A.; Lu, F.; Baltruschat, H.; Schardt, B. C.; Stickney, J. L.;  
4 Soriaga, M. P.; Frank, D. G.; Hubbard, A. T. Structure and composition of a platinum(111)  
5 surface as a function of pH and electrode potential in aqueous bromide solutions. *Langmuir*  
6 **1986**, *2*, 828-835.
- 7 (19) Lucas, C. A.; Markovic, N. M.; Ross, P. N. Observation of an ordered bromide  
8 monolayer at the Pt(111)- solution interface by in-situ surface X-ray scattering. *Surf. Sci.* **1995**,  
9 *340*, L949-L954.
- 10 (20) Gasteiger, H. A.; Markovic, N. M.; Ross, P. N. Bromide adsorption on Pt(111):  
11 Adsorption isotherm and electrosorption valency deduced from RRD(Pt(111))E measurements.  
12 *Langmuir* **1996**, *12*, 1414-1418.
- 13 (21) Orts, J. M.; Gómez, R.; Feliu, J. M.; Aldaz, A.; Clavilier, J. Voltammetry, charge  
14 displacement experiments, and scanning tunneling microscopy of the Pt(100)-Br system.  
15 *Langmuir* **1997**, *13*, 3016-3023.
- 16 (22) Garcia-Araez, N.; Climent, V.; Herrero, E.; Feliu, J.; Lipkowski, J.  
17 Thermodynamic studies of bromide adsorption at the Pt(111) electrode surface perchloric acid  
18 solutions: Comparison with other anions. *J. Electroanal. Chem.* **2006**, *591*, 149-158.
- 19 (23) Tanaka, S.; Yau, S. L.; Itaya, K. In-situ scanning tunneling microscopy of bromine  
20 adlayers on Pt(111). *J. Electroanal. Chem.* **1995**, *396*, 125-130.
- 21 (24) Bertel, E.; Schwaha, K.; Netzer, F. P. The adsorption of bromine on Pt(111):  
22 Observation of an irreversible order-disorder transition. *Surf. Sci.* **1979**, *83*, 439-452.
- 23 (25) Korzeniewski, C.; Climent, V.; Feliu, J. M. *Electrochemistry at Platinum Single*  
24 *Crystal Electrodes. In Electroanalytical Chemistry: A Series of Advances*; Bard, A. J., Zoski, C.,  
25 Eds.; CRC Press: Boca Raton, 2012; Vol. 24; pp 75-169.
- 26 (26) Clavilier, J.; Armand, D.; Sun, S. G.; Petit, M. Electrochemical adsorption  
27 behaviour of platinum stepped surfaces in sulphuric acid solutions *J. Electroanal. Chem.* **1986**,  
28 *205*, 267-277.
- 29 (27) Climent, M. A.; Valls, M. J.; Feliu, J. M.; Aldaz, A.; Clavilier, J. The behavior of  
30 platinum single-crystal electrodes in neutral phosphate buffered solutions. *J. Electroanal.*  
31 *Chem.* **1992**, *326*, 113-127.
- 32 (28) Gisbert, R.; García, G.; Koper, M. T. M. Adsorption of phosphate species on  
33 poly-oriented Pt and Pt(111) electrodes over a wide range of pH. *Electrochim. Acta* **2010**, *55*,  
34 7961-7968.
- 35 (29) Briega-Martos, V.; Herrero, E.; Feliu, J. M. Effect of pH and water structure on  
36 the oxygen reduction reaction on platinum electrodes. *Electrochim. Acta* **2017**, *241*, 497-509.
- 37 (30) Chen, X.; McCrum, I. T.; Schwarz, K.; Janik, M. J.; Koper, M. T. M. Co-adsorption  
38 of cations as the cause of the apparent pH dependence of hydrogen adsorption on a stepped  
39 platinum single-crystal electrode. *Angew. Chem. Int. Ed.* **2017**, *56*, 15025-15029.
- 40 (31) Yaguchi, M.; Uchida, T.; Motobayashi, K.; Osawa, M. Speciation of adsorbed  
41 phosphate at gold electrodes: A combined surface-enhanced infrared absorption spectroscopy  
42 and DFT study. *J. Phys. Chem. Lett.* **2016**, *7*, 3097-3102.
- 43 (32) Garcia-Araez, N.; Climent, V.; Herrero, E.; Feliu, J. M.; Lipkowski, J.  
44 Thermodynamic approach to the double layer capacity of a Pt(111) electrode in perchloric acid  
45 solutions. *Electrochim. Acta* **2006**, *51*, 3787-3793.
- 46 (33) Garcia-Araez, N.; Climent, V.; Rodriguez, P.; Feliu, J. M. Elucidation of the  
47 chemical nature of adsorbed species for Pt(111) in H<sub>2</sub>SO<sub>4</sub> solutions by thermodynamic analysis.  
48 *Langmuir* **2010**, *26*, 12408-12417.
- 49 (34) Climent, V.; Attard, G. A.; Feliu, J. M. Potential of zero charge of platinum  
50 stepped surfaces: a combined approach of CO charge displacement and N<sub>2</sub>O reduction. *J.*  
51 *Electroanal. Chem.* **2002**, *532*, 67-74.
- 52 (35) Weaver, M. J. Potentials of zero charge for platinum(111)-aqueous interfaces:  
53 A combined assessment from in-situ and ultrahigh-vacuum measurements. *Langmuir* **1998**, *14*,  
54 3932-3936.
- 55  
56  
57  
58  
59  
60

1  
2  
3 (36) Climent, V.; Garcia-Araez, N.; Herrero, E.; Feliu, J. Potential of zero total charge  
4 of platinum single crystals: A local approach to stepped surfaces vicinal to Pt(111). *Russ. J.*  
5 *Electrochem.* **2006**, *42*, 1145-1160.

6 (37) Attard, G. A.; Hazzazi, O.; Wells, P. B.; Climent, V.; Herrero, E.; Feliu, J. M. On  
7 the global and local values of the potential of zero total charge at well-defined platinum  
8 surfaces: stepped and adatom modified surfaces. *J. Electroanal. Chem.* **2004**, *568*, 329-342.

9 (38) Martinez-Hincapie, R.; Sebastian-Pascual, P.; Climent, V.; Feliu, J. M.  
10 Investigating interfacial parameters with platinum single crystal electrodes. *Russ. J.*  
11 *Electrochem.* **2017**, *53*, 227-236.

12 (39) Garcia-Araez, N.; Climent, V.; Herrero, E.; Feliu, J. M.; Lipkowski, J.  
13 Determination of the Gibbs excess of H adsorbed at a Pt(111) electrode surface in the  
14 presence of co-adsorbed chloride. *J. Electroanal. Chem.* **2005**, *582*, 76-84.  
15  
16  
17  
18  
19  
20  
21  
22  
23  
24  
25  
26  
27  
28  
29  
30  
31  
32  
33  
34  
35  
36  
37  
38  
39  
40  
41  
42  
43  
44  
45  
46  
47  
48  
49  
50  
51  
52  
53  
54  
55  
56  
57  
58  
59  
60

## TOC GRAPHIC

